

Supporting Information

PPDO/PCL/PEG Based Amphiphilic Polyurethanes with Controllable Degradation and Mechanical Retention

Yue Chen¹, Qi Wang¹, Yuan Bai², Jing Li^{1*}, Nan Zhang³, Bin He^{1*}

¹ National Engineering Research Center for Biomaterials, College of Biomedical Engineering, Sichuan University, Cheng du 610064, China

² Ningbo Baoting Biotechnology LTD, Ningbo 315000, China

³ Institute of Organoid on Chip and Drug Translation Research, Henan Academy of Sciences, Zhengzhou 450046, China

* Corresponding authors, E-mail: sakura-blossoms@foxmail.com (Dr J. Li)
bhe@scu.edu.cn (Dr. Bin He)

Table S1. MLLass fractions of each component calculated from the ¹H NMR spectrum.

Name	PCL (wt%)	PPDO-PEG-PPDO (wt%)	PEG (2000 g/mol) (wt%)	Total PEG (wt%)
PDEU _{1.5}	36.3	37.0	26.7	39.0
PDEU _{3.5}	45.4	23.8	30.8	38.7
PDEU _{5.5}	50.7	15.7	33.6	38.8

Table S2. T_a and Mass fractions of each component estimated from TG and DTG curves.

Name	T _a (°)	PPDO wt%	PCLwt%	PEG wt%	PPDO:PCL
PDEU _{1.5}	245.8	23.7	34.5	40.9	1:1.5
PDEU _{3.5}	236.8	13.1	45.8	40.7	1:3.5
PDEU _{5.5}	266.2	8.7	48.0	40.0	1:5.5

Table S3. Body weight changes of experimental rats at different time points during subcutaneous implantation.

Sample/Mass (g)	Implantation Time (Week)				
	0	1	4	7	10
1	253	320			
2	300	335			
3	306	334			
4	232	277	379		
5	183	210	330		
6	179	219	241		
7	313	346	441	485	
8	262	302	379	430	
9	186	227	341	380	
10	232	280	362	397	436
11	223	270	362	403	403
12	179	217	258	306	355

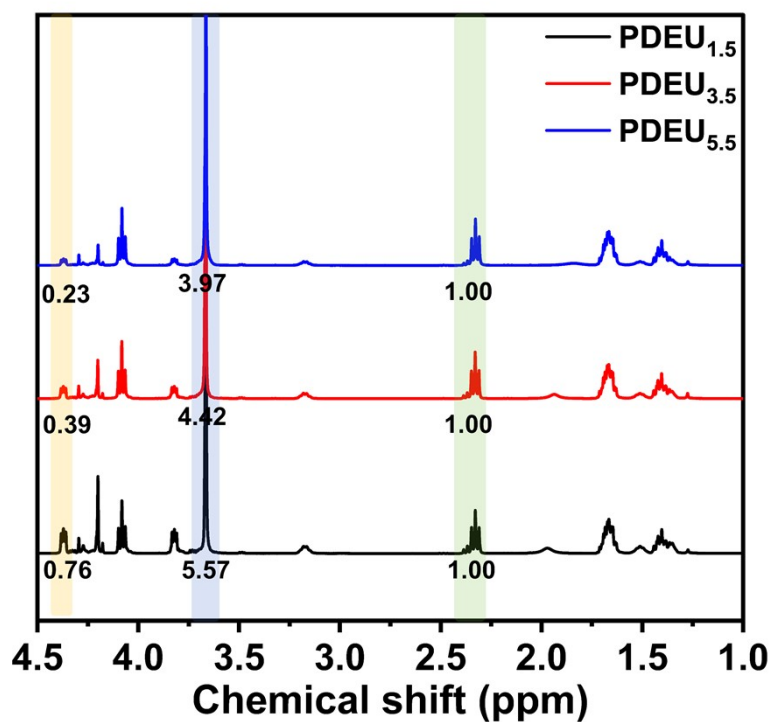


Figure S1. ^1H NMR spectra and characteristic peak integrals (determined using MestReNova software) of PDEU_{1.5}, PDEU_{3.5}, and PDEU_{5.5} at the initial degradation stage (day 0).

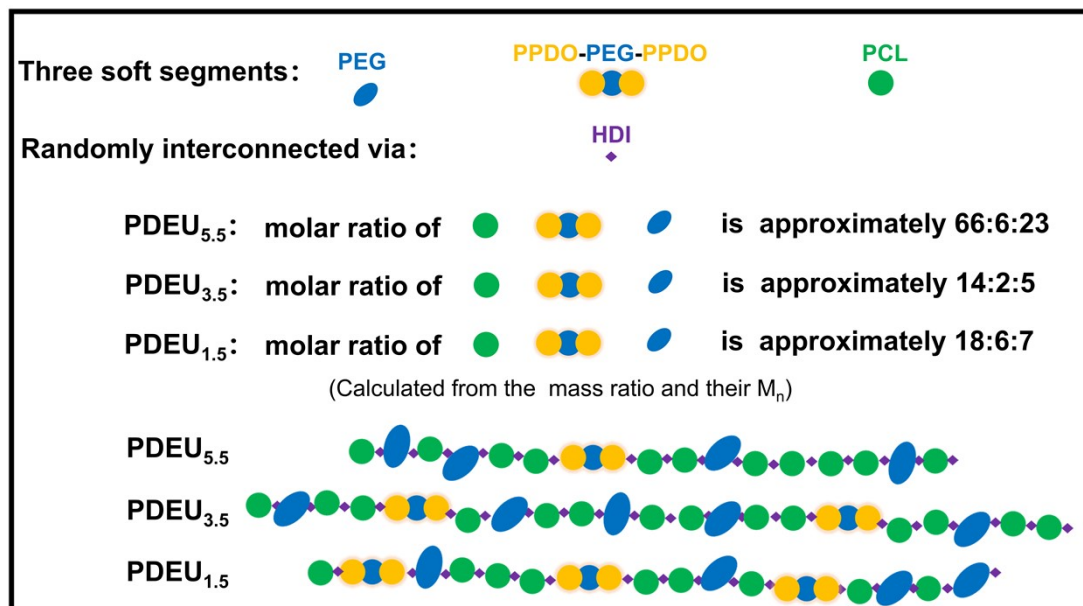


Figure S2. Schematic illustration of the structures of PDEU_{1.5}, PDEU_{3.5}, and PDEU_{5.5}.

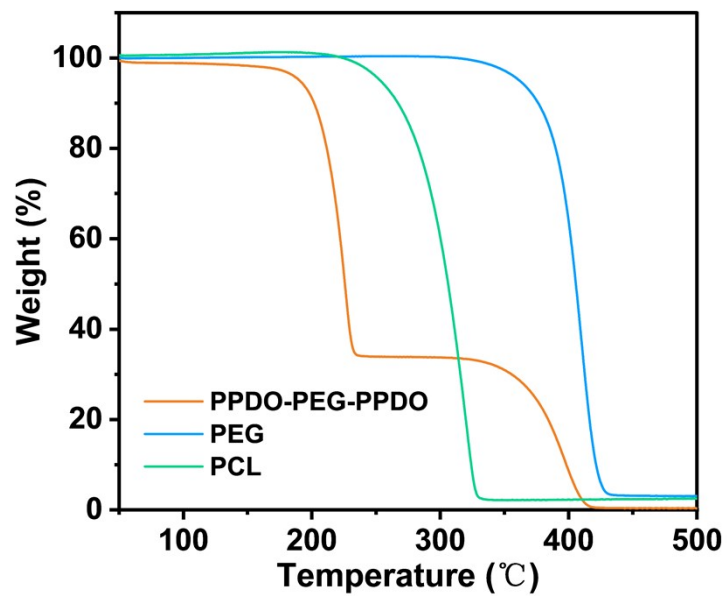


Figure S3. TG curves of PPDO-PEG-PPDO, PCL₁₀₀₀, and PEG₂₀₀₀.

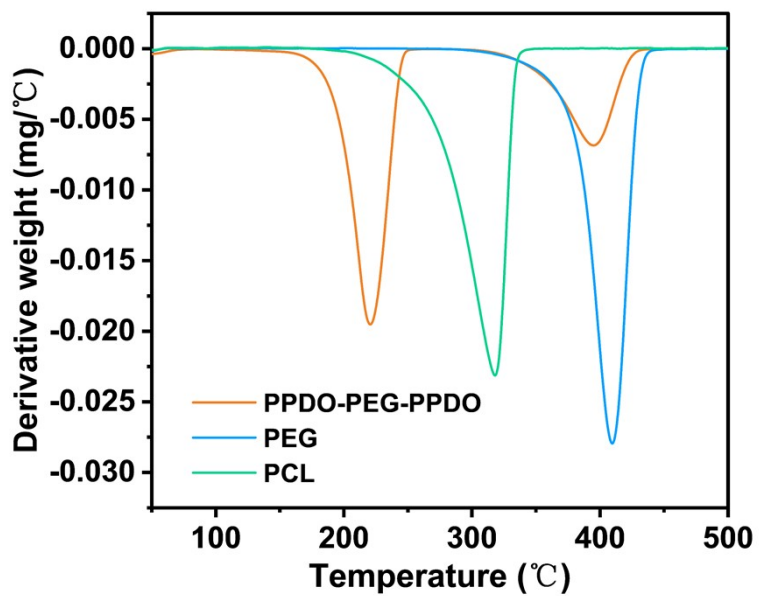


Figure S4. DTG curves of PPDO-PEG-PPDO, PCL₁₀₀₀, and PEG₂₀₀₀.

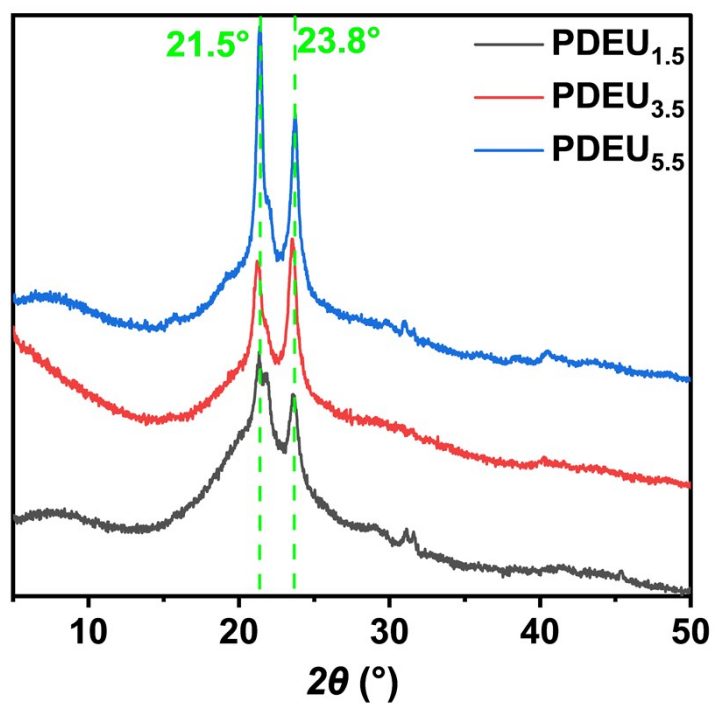


Figure S5. XRD patterns of PDEUs at terminal degradation points (PDEU_{1.5} at day 54, PDEU_{3.5} at day 90, PDEU_{5.5} at day 156).

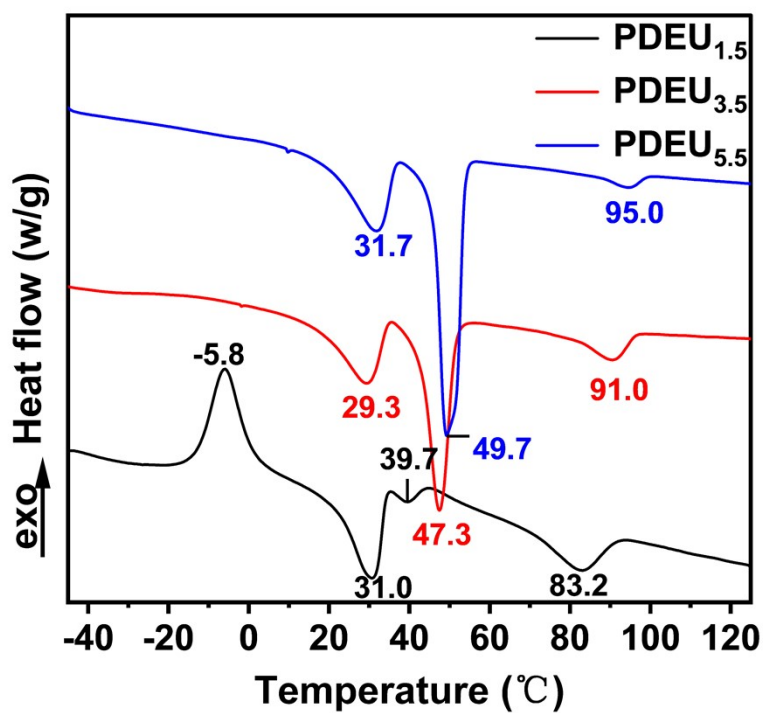


Figure S6. Second Heating DSC Curves of PDEUs at terminal degradation points

(PDEU_{1.5} at day 54, PDEU_{3.5} at day 90, PDEU_{5.5} at day 156).

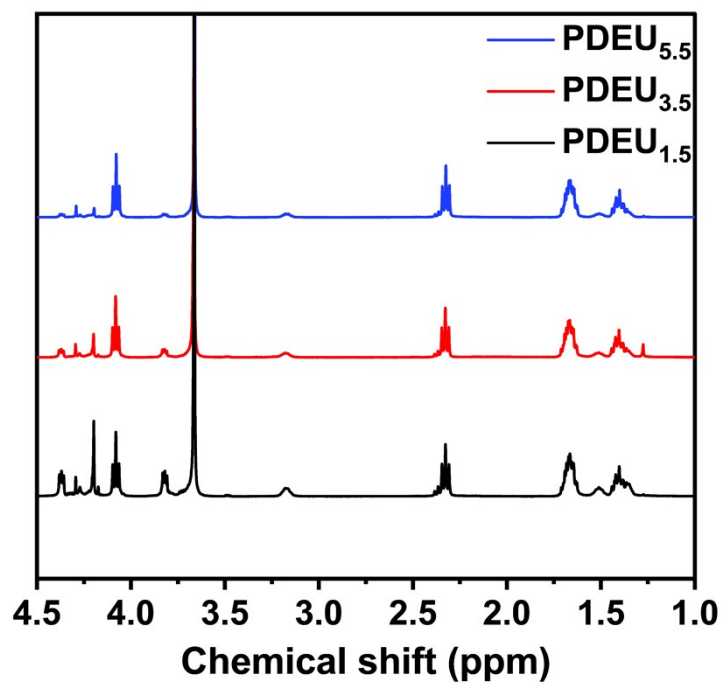


Figure S7. ¹H NMR Spectra of PDEUs at terminal degradation points (PDEU_{1.5} at day 54, PDEU_{3.5} at day 90, PDEU_{5.5} at day 156).

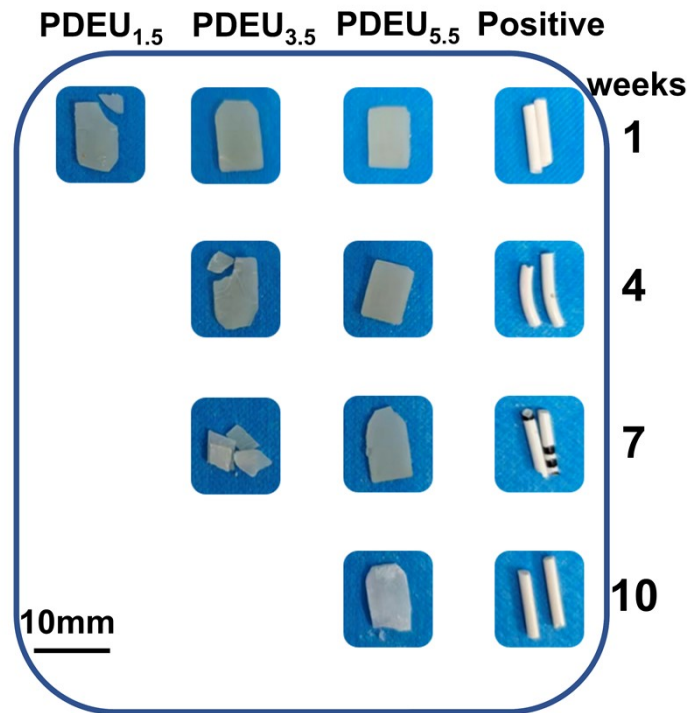


Figure S8. Macroscopic morphologies of PDEUs and mass-matched commercial polyurethane-based ureteral stents (positive control) retrieved at different time points (1, 4, 7, and 10 weeks) after subcutaneous implantation in rats.

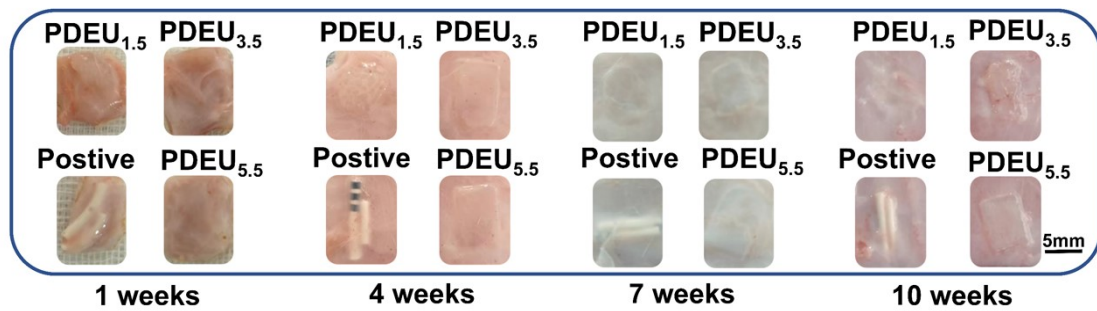


Figure S9. Macroscopic morphologies of the materials and surrounding skin tissues on the dorsal region of rats at different time points.

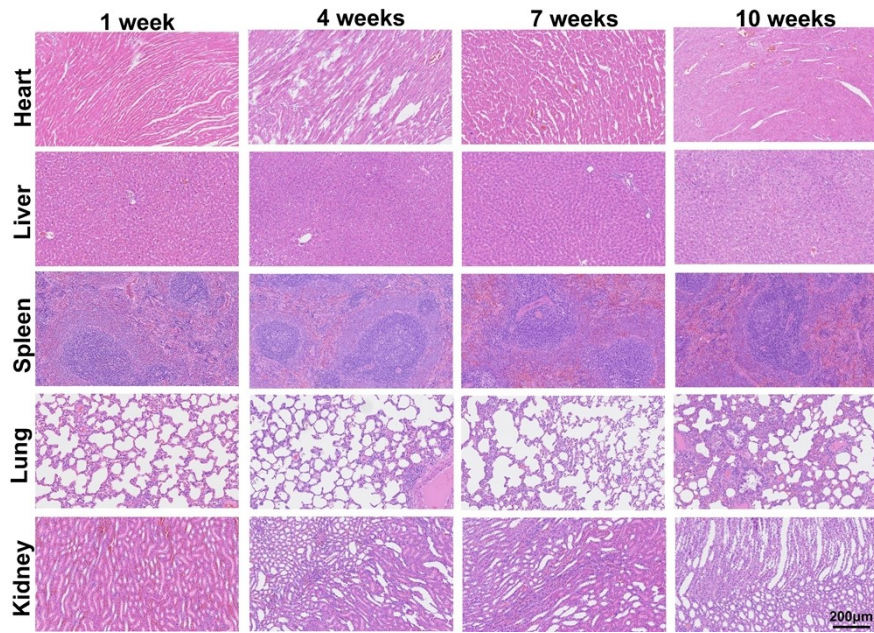


Figure S10. H&E-stained sections of major organs in rats at different time points during the subcutaneous implantation experiment.